WACV 2026 TUCSON, AZ 3/6 -3/10

UNIVERSITY OF CHEMISTRY AND TECHNOLOGY PRAGUE

CTU CZECH TECHNICAL UNIVERSITY IN PRAGUE

Identity Verification from Human Scent using Channel Representation of 2D Gas Chromatography-Mass Spectrometry

Radim Spetlik[1] Jan Hlavsa [1] Jana Cechova[2] Petra Pojmanova[2]
Jiri Matas[1] Stepan Urban[2]

[1]Czech Technical University in Prague (CTU), Faculty of Electrical Engineering
[2]University of Chemistry and Technology, Prague (UCT Prague)

March 2026

Why Scent Biometrics?

- **Individuals emit** distinctive **scent signatures** remaining stable over time [1, 2].
- Does **not require** subject's active **participation** or **direct line of sight**.
- **Withstand** environmental **noise** from various sources [3–6].
- **Persists over time** on collected traces, enabling **delayed acquisition** and re-analysis [1, 2].
- Can be potentially **sampled at a distance** using electronic noses [7, 8].

GC×GC–ToF-MS I

- An **analytical technique** that **separates and identifies chemical compounds** in complex gas mixtures.
- **Two columns** in series (capillary tubes) with different stationary phases → complementary (often near-orthogonal) separations.
  - 1st. dim. (t_1) – first column
  - A periodic modulator (T_{mod}) slices the t_1 effluent and injects it into a faster second column.
  - 2nd. dim. ($t_2 \in [0, T_{mod})$) – second column
- A **binary mask** is applied to ensure **uniform dimensions** and suppress **acquisition artifacts** (e.g., solvent tailing).

- **Pixel grid:**
  $\Omega = \{1, \ldots, H\} \times \{1, \ldots, W\}$,
  $\mathbf{u} = (u_1, u_2) \in \Omega$
- **Measurement:**
  $\mathcal{S} = \{s(\mathbf{u})\}_{\mathbf{u} \in \Omega}$
- **Local spectrum**:
  $s(\mathbf{u}) = \{(m_{n,\mathbf{u}},\ I_{n,\mathbf{u}})\}_{n=1}^{N(\mathbf{u})}$,

  where $m_{n,\mathbf{u}}$ is the mass-to-charge ratio (m/z) and $I_{n,\mathbf{u}}$ its intensity.

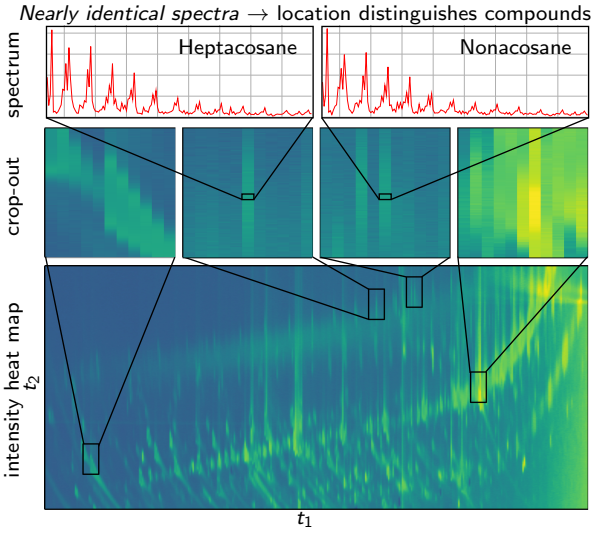

Figure 1: Intensity heat map of the mass detector.

Human Scent Dataset (HSD) I

- **2528 samples** from **252 individuals**.
  - 4D-C (published): 504 samples, 40 individuals [9].
  - 129 male identities – 1 178 samples
  - 123 female identities – 1 350 samples
- Two different **ToF-MS** detectors:
  - **Pegasus® 4D-C** 10-bit values.
  - **Pegasus® BT 4D** floating-point values.

Detector	Samples total:	n	Samples per identity min	max	avg	med.
4D-C	1341	116	1	76	11.6	10
BT 4D	1187	139	2	34	8.5	9

Table 1: Human Scent Dataset statistics.
n - number of identities

Dataset	Samples total:	n	Samples per identity min	max	avg	med.
4D-C	504	40	10	37	12.6	10
HSD	2528	252	1	76	10.0	10

Table 2: HSD vs. 4D-C. datasets.
n - number of identities

Human Scent Dataset (HSD) II

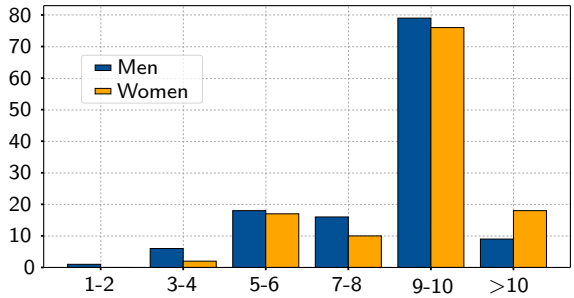

Figure 2: Histogram of measurement counts per identity in the HSD dataset, grouped by biological sex. X-axis: measurements per identity, y-axis: number of subjects.

- We compress the raw mass spectra $s(\mathbf{u})$ with a bank of C **overlapping, learnable basis functions**:

$$\phi_k(m_{n,\mathbf{u}}) = \alpha_k \, \kappa(m_{n,\mathbf{u}}; \theta_k)$$

- We convert $\mathcal{S}$ to a *channel-encoded image* $\mathbf{C} \in \mathbb{R}^{C \times H \times W}$:

$$\mathbf{C}_{k,\mathbf{u}} = \sum_{n=1}^{N(\mathbf{u})} \phi_k(m_{n,\mathbf{u}}) \, I_{n,\mathbf{u}}$$

- **Training (self-supervised):** learn $\{\alpha_k, \theta_k\}$ by weighted MSE reconstruction

$$E = \sum_{\mathbf{u} \in \Omega} \sum_{n=1}^{N(\mathbf{u})} \frac{1}{w_{n,\mathbf{u}}} \left(I_{n,\mathbf{u}} - \hat{I}_{n,\mathbf{u}} \right)^2.$$

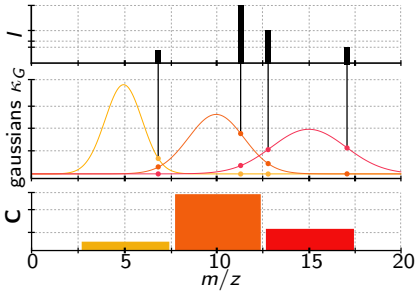

Figure 3: Toy example of a single local spectrum $s(\mathbf{u})$ encoded with $C = 3$ gaussian kernels used as basis functions for channel representation.

Registration vs. Non Registration

- **Instrument factors**, such as temperature changes or hardware drift, **can shift retention times** across a GC×GC–ToF-MS measurement, leading to misaligned compounds and unreliable comparisons [9].
- We experimented with both with and without registration.
- The proposed registration method [9]:
  1. Chemical compound peak detection - detect position $\hat{\mathbf{u}}_c^{(\mathcal{S})}$ using reference mass spectrum $\bar{\mathbf{s}}_c$ compound peak detectors $c_{\cos}(\bar{\mathbf{u}}_c, \bar{\mathbf{s}}_c)$ or $\mathrm{FCN}(\mathbf{u}, \mathbf{s})^{+}_{\cos}$ [9].
  2. Delaunay triangulation - over the estimated locations $\{\hat{\mathbf{u}}_c^{(\mathcal{S})}\}$
  3. Coordinate transformation – barycentric interpolation, mapping estimated $\hat{\mathbf{u}}_c^{(\mathcal{S})}$ to the reference location $\mathbf{u}_c$.
  4. Piecewise-linear interpolation – original measurement is interpolated to produce a canonical grid.

Verification Pipeline

- **Learnable Embedding:** $f : \mathbb{R}^{C\times H\times W} \to \mathbb{R}^D$
  - For CNN-based f, we train with margin-based triplet loss:

$$\mathcal{L}(f, d, \gamma) = \frac{1}{|\mathcal{T}|} \sum_{(a,p,n)\in\mathcal{T}} \max\{d_{ap} - d_{an} + \gamma, 0\}$$

- **Dissimilarity:** $d : \mathbb{R}^D \times \mathbb{R}^D \to \mathbb{R}_{\geq 0}$ (e.g. cosine)
- **Pairwise score:**

$$d_{ij} := d\big(f(\mathbf{C}_i),\, f(\mathbf{C}_j)\big)$$

- **Decision (test time):**

$$y_{ij} := [\![\, d_{ij} < \tau \,]\!]$$

  - $y_{ij} = 1$: same identity, $y_{ij} = 0$: different identities

Embedding Function f

We experimented with different embedding functions:

- Hand-engineered descriptors: LBP [10], HOG [11],SIFT [12]
- 5 pretrained backbones followed by a lightweight projection layer: *ResNet-18* [13], *ResNet-101* [13], *VGG-16* [14], *Inception-v3* [15], *GoogLeNet* [15]
- Custom-designed CNN consisting of 3 modules:
  1. convolutional backbone using anisotropic 2×8 kernel (reflecting the structure of the input data)
  2. downsampling stack
  3. residual multi-layer perceptron head

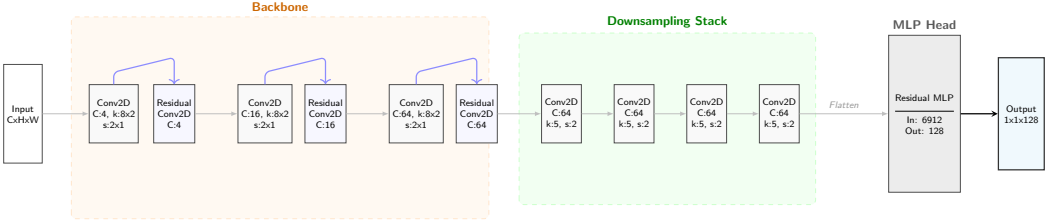

Results I

- **Scent signatures can serve as a biometric** trait when processed with modern feature embedding techniques.
- Achieving **89.5 ± 3.4 AUROC** and **53.3 ± 8.3 TPR@5%** using custom-designed CNN and 10-fold cross-validation.
- Using **CNN** as an embedding function f **outperforms** both **standard approach** in chemistry and traditional descriptors.
- Explicit **spatial registration** (alignment) of the chemical samples was found **not** to be **necessary**.
- **Anisotropic** 2×8 **kernels** in the **custom CNN** improved performance, better matching the structure of GC×GC–ToF-MS data; **standard pretrained backbones** remain **competitive**.

Results II

				$c_{\cos}(\bar{\mathbf{u}}_c, \bar{\mathbf{s}}_c)$				$\mathrm{FCN}(\mathbf{u}, \mathbf{s})^{+}_{\cos}$			
		no registration		$\mathcal{R}^{(22)}$		$\mathcal{R}^{(24)}$		$\mathcal{R}^{(22)}$		$\mathcal{R}^{(24)}$	
	C	AUROC	TPR@5%	AUROC	TPR@5%	AUROC	TPR@5%	AUROC	TPR@5%	AUROC	TPR@5%
baseline	–	79.3 ± 6.2	42.0 ± 12.6	–	–	–	–	–	–	–	–
HOG	1	73.0 ± 6.6	39.1 ± 7.8	74.3 ± 7.2	39.1 ± 7.8	74.4 ± 7.3	39.3 ± 7.7	76.0 ± 4.9	33.4 ± 7.2	76.7 ± 5.0	33.8 ± 7.1
LBP	1	78.1 ± 3.2	15.8 ± 2.2	77.1 ± 2.8	15.8 ± 2.2	77.1 ± 2.8	15.5 ± 2.1	76.8 ± 4.0	22.4 ± 4.3	78.1 ± 4.3	22.9 ± 4.9
SIFT	1	66.6 ± 6.0	18.6 ± 5.3	63.8 ± 4.1	15.5 ± 4.0	63.4 ± 3.9	15.1 ± 3.8	59.0 ± 6.7	13.4 ± 4.0	63.8 ± 6.5	17.4 ± 4.9
VGG16	3	77.0 ± 4.6	40.5 ± 6.6	79.5 ± 9.6	42.9 ± 10.4	79.8 ± 9.4	42.2 ± 9.4	74.6 ± 7.2	26.2 ± 8.3	74.5 ± 6.9	26.6 ± 6.6
ResNet-18	3	87.5 ± 3.9	44.9 ± 8.8	87.3 ± 3.5	42.9 ± 5.2	86.9 ± 3.0	41.1 ± 5.9	85.2 ± 3.8	36.1 ± 7.1	85.5 ± 4.3	36.2 ± 8.2
ResNet-101	3	86.3 ± 4.1	41.5 ± 11.4	86.0 ± 4.2	38.5 ± 8.7	86.5 ± 4.1	40.6 ± 7.7	84.5 ± 4.7	35.3 ± 8.7	84.9 ± 4.4	35.2 ± 9.1
GoogLeNet	3	87.9 ± 3.5	46.8 ± 7.7	86.8 ± 3.9	44.3 ± 8.4	86.7 ± 3.4	44.7 ± 7.5	85.0 ± 3.8	35.2 ± 8.9	84.9 ± 4.1	36.1 ± 10.3
Inception-v3	3	86.0 ± 3.5	40.2 ± 5.6	85.5 ± 3.3	39.2 ± 5.0	85.5 ± 3.5	40.2 ± 5.1	83.5 ± 3.9	32.8 ± 6.8	84.0 ± 4.0	34.3 ± 9.1
custom CNN	5	**89.5** ± 3.4	**53.3** ± 8.3	88.3 ± 3.4	51.3 ± 6.5	88.4 ± 3.4	50.7 ± 6.7	85.8 ± 3.4	46.5 ± 5.5	85.4 ± 3.8	43.9 ± 6.2

Table 3: Performance comparison of five spatial-alignment strategies and ten embedding functions using 10-fold cross-validation. Methods include: (i) chemist baseline [16], (ii) hand-crafted descriptors (LBP, HOG, SIFT), (iii) custom CNN, and (iv) pretrained backbones (ResNet, VGG, Inception, GoogLeNet) with a learned projection.

Limitations

- Accuracy well bellow that of established modalities (iris, fingerprint, face).
- External validity across labs, climates, diets, hygiene, medications, and environments, remains to be investigated.
- Long-term permanence and month-scale drift are un-quantified.
- The observation that explicit canonical registration is unnecessary is currently demonstrated only on Human Scent Dataset, with robustness under stronger retention-time drift and in settings requiring chemical interpretability still to be evaluated.

Thank you for your attention

Project Page

References I

[1] L. Pinc, L. Bartoš, A. Reslová, and R. Kotrba, "Dogs Discriminate Identical Twins," *PLoS ONE*, vol. 6, no. 6, e20704, 2011.

[2] D. J. Penn et al., "Individual and gender fingerprints in human body odour," *Journal of The Royal Society Interface*, vol. 4, no. 13, pp. 331–340, 2006. DOI: 10.1098/rsif.2006.0182.

[3] L. Pinc, L. Bartos, and P. Vyplelova, "Resistance of human odours to extremely high temperature as revealed by trained dogs," *Czech Journal of Animal Science*, vol. 61, no. 4, pp. 172–176, 2016. DOI: 10.17221/8848-CJAS.

[4] R. Peters, R. Veenstra, K. Heutinck, A. Baas, S. Munniks, and J. Knotter, "Human scent characterization: A review," *Forensic Science International*, vol. 349, p. 111 743, 2023.

References II

[5] R. A. Stockham, D. L. Slavin, and W. Kift, "Survivability of human scent," *Forensic Science Communications*, vol. 6, no. 4, 2004, Publisher: Federal Bureau of Investigation.

[6] N. Ladislavová, P. Pojmanová, P. Vrbka, J. Šnupárková, and Š. Urban, "Human scent signature on cartridge case survives gun being fired: A preliminary study on a potential of scent residues as an identification tool," *PLOS ONE*, vol. 18, no. 3, e0283259, 2023.

[7] I. Rodriguez-Lujan, G. Bailador, C. Sanchez-Avila, A. Herrero, and G. Vidal-de-Miguel, "Analysis of pattern recognition and dimensionality reduction techniques for odor biometrics," *Knowledge-Based Systems*, vol. 52, pp. 279–289, 2013, ISSN: 0950-7051. DOI: 10.1016/j.knosys.2013.08.002.

References III

[8] C. Jirayupat et al., "Breath odor-based individual authentication by an artificial olfactory sensor system and machine learning," *Chemical Communications*, vol. 58, no. 44, pp. 6377–6380, 2022, ISSN: 1359-7345. DOI: https://doi.org/10.1039/d1cc06384g.

[9] J. Hlavsa, R. Spetlik, J. Čechová, P. Pojmanová, J. Matas, and Š. Urban, "Sex Classification from Human Scent Using Image Interpretation of 2D Gas Chromatography-Mass Spectrometry Data," in *Image Analysis*, J. Petersen and V. A. Dahl, Eds., Springer Nature Switzerland, 2025, pp. 457–470, ISBN: 978-3-031-95911-0. DOI: 10.1007/978-3-031-95911-0_32.

[10] T. Ojala, M. Pietikainen, and T. Maenpaa, "Multiresolution gray-scale and rotation invariant texture classification with local binary patterns," *IEEE Transactions on pattern analysis and machine intelligence*, vol. 24, no. 7, pp. 971–987, 2002.

References IV

[11] N. Dalal and B. Triggs, "Histograms of oriented gradients for human detection," in *2005 IEEE computer society conference on computer vision and pattern recognition (CVPR'05)*, Ieee, vol. 1, 2005, pp. 886–893.

[12] D. G. Lowe, "Distinctive image features from scale-invariant keypoints," *International journal of computer vision*, vol. 60, no. 2, pp. 91–110, 2004.

[13] K. He, X. Zhang, S. Ren, and J. Sun, "Deep Residual Learning for Image Recognition," in *Proceedings of the IEEE Conference on Computer Vision and Pattern Recognition*, 2016, pp. 770–778. DOI: 10.1109/CVPR.2016.90. Accessed: Jul. 17, 2025.

[14] K. Simonyan and A. Zisserman, "Very Deep Convolutional Networks for Large-Scale Image Recognition," in *Proceedings of 3rd International Conference on Learning Representations*, 2015.

References V

[15] C. Szegedy et al., "Going deeper with convolutions," in *Proceedings of IEEE Conference on Computer Vision and Pattern Recognition*, Jun. 2015, pp. 1–9. DOI: 10.1109/CVPR.2015.7298594.

[16] V. Cuzuel et al., "Human odor and forensics: Towards Bayesian suspect identification using GC×GC–MS characterization of hand odor," *Journal of Chromatography B*, vol. 1092, pp. 379–385, 2018, ISSN: 1570-0232. DOI: 10.1016/j.jchromb.2018.06.018.